Asian Journal of Chemistry; Vol. 38, No. 8 (2026), 2125-2130
ASIAN JOURNAL OF CHEMISTRY
https://doi.org/10.14233/ajchem.2026.36231

Cobalt Loading-Dependent Performance of Co/SiO_2 Catalysts for the Selective Dehydrogenation of 1,4-Butanediol to γ-Butyrolactone

K. RAJENDRA PRASAD*, and J. MADHUSUDANA RAO*,

Division of Natural Products Chemistry, CSIR-Indian Institute of Chemical Technology, Hyderabad-500007, India

*Corresponding authors: E-mail: rajendraprasad.kothakonda@gmail.com; jmrnpl@yahoo.com

Received: 16 April 2026 *Accepted*: 10 July 2026 *Published online*: 7 August 2026 AJC-22439

Cobalt-supported catalysts (Co/SiO_2) of different metal loadings (5-15 wt.%) were developed and assessed for the vapour-phase dehydrogenation of 1,4-butanediol to γ-butyrolactone and tetrahydrofuran. Catalysts were also systematically characterised by N_2 physisorption, X-ray diffraction and H_2 temperature-programmed reduction (H_2-TPR). BET studies illustrated a gradual decrease of the total specific surface area with cobalt loading due to possible clogging of the pores by cobalt oxides species. XRD confirmed the formation of crystallised Co_3O_4 phases with higher loadings leading to larger crystallite sizes. H_2-TPR profiles confirmed better reducibility and lower metal-support interaction at elevated cobalt loadings. Catalytic analysis showed an increase of 1,4-butanediol conversion and 1,4-butanediol selectivity with reaction temperature and cobalt loading, with the highest conversion (80%) obtained at 580 K using a $15Co/SiO_2$ catalyst. Time-on-stream experiments demonstrated good stability of the catalyst with only negligible deactivation observed during 7 h continuous operation. High cobalt loading significantly enhanced the catalytic activity of Co/SiO_2 catalysts by increasing the number of reducible cobalt species and the availability of accessible metallic active sites. These findings demonstrate that high-loading Co/SiO_2 catalysts are highly promising for the green and atom-economical dehydrogenation of biomass-derived diols.

Keywords: 1,4-Butanediol, Co/SiO_2 catalyst, Dehydrogenation, γ-Butyrolactone, Fixed-bed reactor.

INTRODUCTION

With the increasing focus on sustainable chemistry, studies on catalytic upgrading of biomass-derived platform molecules to value-added chemicals has significantly grown [1,2]. Among these molecules, 1,4-butanediol is a versatile diol that can be selectively converted into γ-butyrolactone or tetrahydrofuran used in the production of polymers, pharmaceuticals and specialty solvents. Oxidant-free catalytic dehydrogenation of 1,4-butanediol is an attractive and atom-economical route that proceeds under relatively mild conditions while producing hydrogen as the sole byproduct, making it a sustainable approach for the synthesis of value-added chemicals [3,4].

Supported metal-based catalysts, especially Cu-based systems on SiO_2 and mixed oxides, have been shown to be highly active in this transformation and catalytic performance is mainly dependent on the metal dispersion, particle size as well as the redox properties of the surface [4-6]. Mechanistic studies indicate that the reaction advances through a series of dehydrogenation and cyclisation steps with 4-hydroxybutanal being the most important intermediate [5]. While noble metal catalysts including Au- and Ru-based systems show improved yield and selectivity, they are often too expensive and scarce to be used at an industrial scale [7]. Accordingly, cobalt- and copper-based transition metal catalysts have attracted considerable attention as cost-effective alternatives to noble metal catalysts, offering comparable catalytic performance while significantly reducing material costs. Bimetallic formulations and defect engineering in catalyst design were also implemented to achieve higher catalytic activity *via* improved metal dispersion and synergistic electronic effects [6-8].

Silica (SiO_2) is one of the widely used catalyst supports, as it has a strength and thermal stability at higher temperatures besides providing high surface area and being chemically inert to ensure homogeneous dispersion of active metal species. The interaction of cobalt with the silica surface plays a crucial role in determining catalyst reducibility, metal dispersion and long-term stability. At cobalt loadings below 30 wt.%, strong metal–support interactions lead to highly dispersed cobalt species, which are relatively difficult to reduce. In contrast,

higher cobalt loadings promote the formation of larger cobalt oxide particles with weaker support interactions, enhancing reducibility and increasing the availability of catalytically active metallic Co^0 sites [4,8].

Despite the reported use of silica-supported cobalt catalysts for 1,4-butanediol dehydrogenation, a systematic understanding of the influence of cobalt loading on catalyst structure, reducibility, dispersion and catalytic performance under identical preparation and reaction conditions remains limited. In this study, a series of Co/SiO_2 catalysts with varying cobalt loadings was synthesised using a consistent protocol to establish structure–activity relationships for the selective dehydrogenation of 1,4-butanediol to γ-butyrolactone. Correlating cobalt loading with the physico-chemical properties and catalytic performance provides valuable guidelines for the rational design of efficient, low-cost cobalt-based catalysts for sustainable biomass conversion.

EXPERIMENTAL

Catalyst preparation: SiO_2 (Merck) was used as the catalyst support and Co/SiO_2 catalysts were prepared by the incipient wetness impregnation method using $Co(NO_3)_2{\cdot}6H_2O$ as the cobalt precursor. An aqueous solution of the precursor was added dropwise to the SiO_2 support under continuous stirring to ensure uniform cobalt distribution. The resulting slurry was evaporated to dryness under mild heating and the solid was dried overnight at 393 K, followed by calcination in flowing air at 723 K for 5 h. Catalysts with cobalt loadings of 5, 10 and 15 wt.% were designated as $5Co/SiO_2$, $10Co/SiO_2$ and $15Co/SiO_2$, respectively.

Characterisation: X-ray diffraction measurements on a Rigaku Ultima IV diffractometer using Cu*K*α radiation (λ = 1.54178 Å), operated at 40 kV and 20 mA, were performed to determine the crystalline phases of the catalysts. Average crystallite sizes were calculated using the following Scherrer's equation:

$$D = \frac{K\lambda}{\beta \cos\theta}$$

where K is Scherrer shape factor (0.9); λ is X-ray wavelength; β is full width at half-maximum (FWHM) of diffraction peak; and θ is Bragg angle; D is the mean crystallite diameter.

The textural properties of the catalysts were determined from N_2 adsorption–desorption isotherms measured at 77 K using a SMART SORB 92/93 analyzer (Smart Instruments, India). Before analysis, the samples were degassed under vacuum at 473 K for 2 h to remove adsorbed moisture and impurities. H_2-temperature-programmed reduction (H_2-TPR) was performed using 50 mg of catalyst under a 5 vol.% H_2/Ar flow (60 mL min^{-1}), with the temperature increased from ambient to 1073 K at 10 ºC min^{-1}, while hydrogen consumption was monitored using a thermal conductivity detector (TCD). Transmission electron microscopy (TEM) was carried out using a JEOL, Switzerland. For TEM analysis, the catalyst was ultrasonically dispersed in ethanol, deposited onto a carbon-coated copper grid and dried at 350 K for 5 h before imaging.

Catalytic reaction procedure: Catalytic dehydrogenation of 1,4-butanediol was carried out at atmospheric pressure in a bench-scale continuous-flow fixed-bed quartz reactor. The catalyst (0.2-0.5 g, particle size 250-500 μm) was packed between quartz wool plugs and reduced *in situ* under 5 vol.% H_2/Ar at 673 K for 2 h to generate the active metallic cobalt phase. After reduction, the reactor was cooled to the desired reaction temperature under a N_2 atmosphere. Liquid 1,4-butanediol was fed using a calibrated syringe pump, vaporized before entering the reactor, and carried by N_2 to ensure a stable reactant flow and effective vapour-catalyst contact. Reactions were performed over the temperature range of 523-593 K. The reaction products were analysed online using gas chromatography (GC-FID) equipped with an HP-5 capillary column, and quantified by external calibration with authentic standards. The 1,4-butanediol conversion and product selectivity were calculated as:

$$\text{Conversion (\%)} = \frac{\text{moles of 1,4-butanediol converted}}{\text{moles of 1,4-butanediol fed}} \times 100$$

$$\text{Selectivity (\%)} = \frac{\text{moles of product formed}}{\text{moles of 1,4-butanediol converted}} \times 100$$

Catalyst stability was evaluated through time-on-stream experiments at optimised conditions up to 12 h of continuous operation.

RESULTS AND DISCUSSION

XRD studies: The crystalline forms of Co/SiO_2 catalysts ($5Co/SiO_2$, $10Co/SiO_2$ and $15Co/SiO_2$) were investigated using XRD with the patterns as shown in Fig. 1. All catalysts exhibit a broad diffraction band at $2\theta \approx 20\text{-}25^\circ$, characteristic of amorphous SiO_2, confirmed that the silica support retains its non-crystalline structure after cobalt incorporation [9-12]. For all cobalt-loaded catalysts, distinct reflections appear at $2\theta \approx 31^\circ$, 36°, 44°, 59° and 65° assignable to the (220), (311), (400), (511) and (440) planes of cubic-spinel Co_3O_4 (JCPDS card no. 43-1003) [13]. The progressive increase in peak intensity and sharpness from $5Co/SiO_2$ to $15Co/SiO_2$ reflects the growth of Co_3O_4 crystallites with increasing cobalt loading. In contrast, the weaker and broader peaks observed for $5Co/SiO_2$ indicate the presence of finely dispersed cobalt

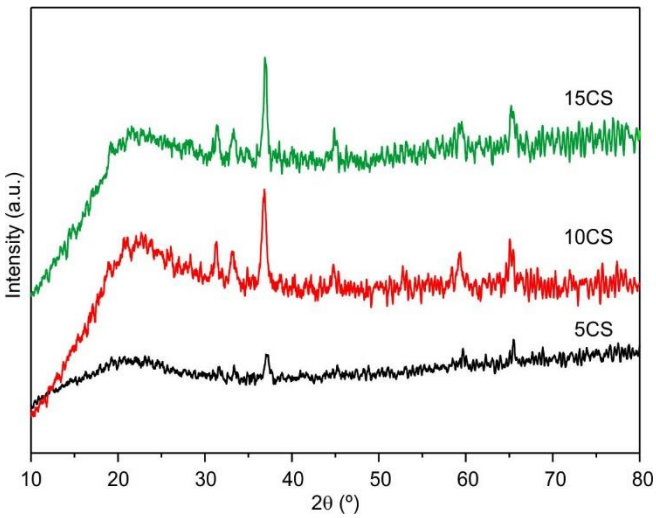

Fig. 1. XRD patterns of Co/SiO_2 catalysts with varying cobalt loadings

oxide species with strong metal–support interactions. At higher cobalt loadings, the sharper reflections suggest the formation of larger Co_3O_4 particles with increased surface aggregation, which can influence catalyst reducibility and the availability of active cobalt sites. No diffraction peaks corresponding to metallic cobalt or impurity phases were detected, confirming the phase purity of the calcined catalysts.

Textural properties: The specific surface areas of the SiO_2 support and the Co/SiO_2 catalysts are summarized in Table-1. The bare SiO_2 support has a specific surface area of 220 $m^2 g^{-1}$. The surface area monotonically decreases with increasing cobalt content: 201, 193 and 177 $m^2 g^{-1}$ for $5Co/SiO_2$, $10Co/SiO_2$ and $15Co/SiO_2$, respectively. This is correlated to the partial blockage of silica mesopores and surface coverage by the growing cobalt oxide clusters. A slight decrease in specific surface area (9 $m^2 g^{-1}$) at 5 wt.% Co suggests the formation of finely dispersed cobalt oxide species that occupy only a small fraction of the silica pores. With increasing cobalt loading, the surface area decreases more markedly (27 $m^2 g^{-1}$), reflecting the growth and partial agglomeration of cobalt oxide particles together with greater pore filling, which reduces nitrogen accessibility during adsorption. Nevertheless, all catalysts retain relatively high surface areas, confirmed that the mesoporous silica framework remains largely preserved. This structural integrity is beneficial for catalysis, as it ensures adequate exposure of active sites while facilitating efficient diffusion of reactants and products.

TABLE-1
BET SURFACE AREA OF SiO_2 AND Co/SiO_2 CATALYSTS

Catalyst	BET surface area ($m^2 g^{-1}$)
SiO_2	220
$5Co/SiO_2$	201
$10Co/SiO_2$	193
$15Co/SiO_2$	177

H_2-TPR analysis: H_2-TPR was used to probe the reducibility of the Co/SiO_2 catalysts and profiles obtained are shown in Fig. 2. Each catalyst shows a major broad reduction peak area in the mid-temperature region which is associated with stepwise reduction of cobalt oxide species ($Co_3O_4 \rightarrow CoO \rightarrow Co^o$) [14]. The asymmetric feature of the profiles proves that these two reduction steps are partially overlapped and suggests a distribution of cobalt species with different metal-support interaction. The progressive increase in the intensity of the reduction peak with increasing cobalt loading demonstrates the presence of a greater amount of reducible cobalt oxide. Among the catalysts, $15Co/SiO_2$ shows the highest and sharpest reduction peak, reflecting the easier reduction of larger, bulk-like Co_3O_4 particles that interact less strongly with the silica support. In contrast, $5Co/SiO_2$ displays a broad, low-intensity reduction peak, consistent with finely dispersed cobalt species, which are strongly bound to the SiO_2 surface and therefore require higher temperatures for complete reduction.

With increasing cobalt loading, the reduction peak shifts to lower temperatures, indicating a gradual weakening of the metal–support interaction and the formation of larger cobalt oxide aggregates. This behaviour facilitates hydrogen activation

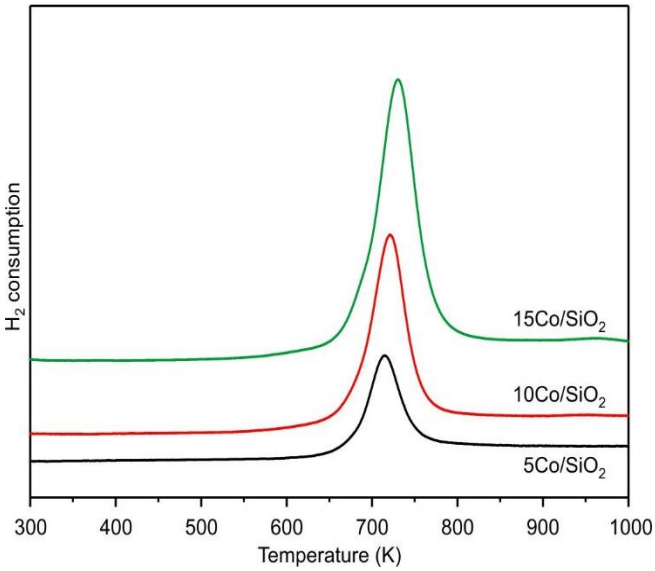

Fig. 2. H_2-TPR profiles of Co/SiO_2 catalysts with varying cobalt loadings

and the generation of metallic Co^o at lower reduction temperatures, which is beneficial for catalytic dehydrogenation. The H_2-TPR results confirm that cobalt loading plays a key role in controlling catalyst reducibility and the strength of the metal–support interaction, both of which strongly influence catalytic performance

TEM studies: The TEM images of the $15Co/SiO_2$ catalyst are shown in Fig. 3. The micrographs reveal agglomerates of nearly spherical cobalt nanoparticles forming a porous network. The cobalt particles are uniformly distributed over the silica support with only moderate aggregation and no large isolated crystallites confirmed good dispersion of the active phase.

Catalytic performance: Dehydrogenation of 1,4-butanediol: The Co/SiO_2 catalysts were evaluated for the vapour-phase dehydrogenation of 1,4-butanediol to γ-butyrolactone and tetrahydrofuran, as illustrated in **Scheme-I**. The reaction proceeds through two competing pathways: γ-butyrolactone is formed *via* sequential dehydrogenation and intramolecular cyclisation, whereas tetrahydrofuran is generated through the dehydration of 1,4-butanediol.

Co/SiO_2 catalysts were investigated for the vapour-phase dehydrogenation of 1,4-butanediol to γ-butyrolactone and tetrahydrofuran as shown in **Scheme-I**. γ-Butyrolactone is formed through sequential dehydrogenation followed by intramolecular cyclisation, whereas tetrahydrofuran is produced *via* a competing dehydration pathway.

Effect of reaction temperature: Fig. 4a shows the effect of reaction temperature (523-593 K) on the conversion of 1,4-butanediol over the Co/SiO_2 catalysts. The conversion increases steadily with temperature for all catalysts, consistent with the endothermic nature of the dehydrogenation reaction. At 580 K, $15Co/SiO_2$ achieves the highest conversion (80%), followed by $10Co/SiO_2$ (70%) and $5Co/SiO_2$ (65%). The superior performance of $15Co/SiO_2$ is attributed to its higher reducibility and better availability of metallic Co^o active sites. The larger Co_3O_4 crystallites observed by XRD are more readily reduced to metallic cobalt, facilitating C–H and O–H bond activation during dehydrogenation. In contrast, the lower

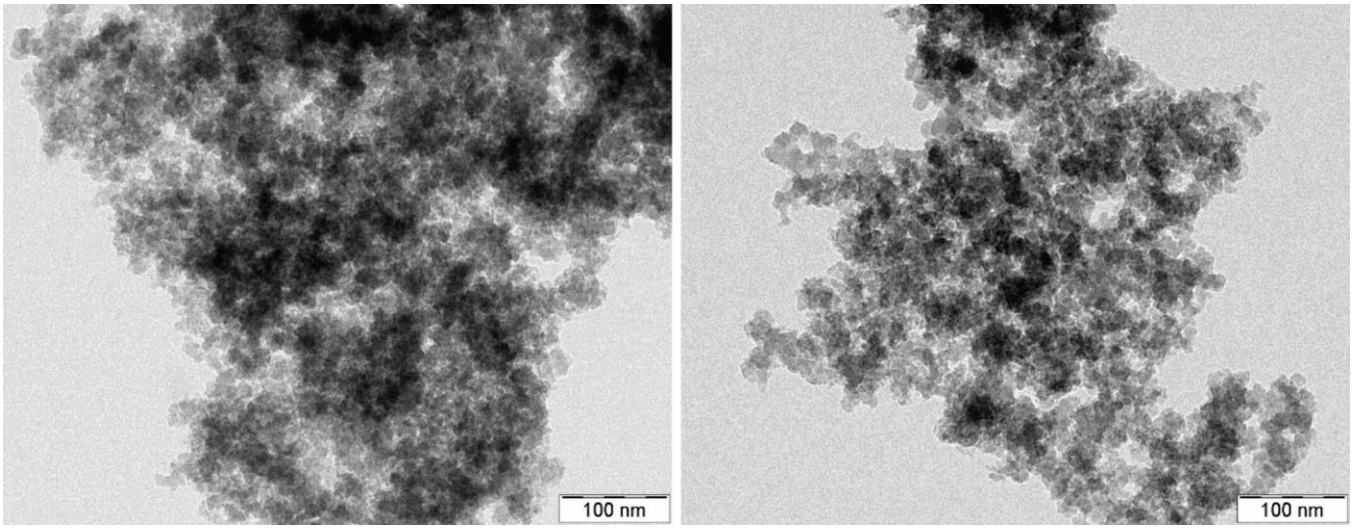

Fig. 3. TEM images of 15Co/SiO_2 catalyst

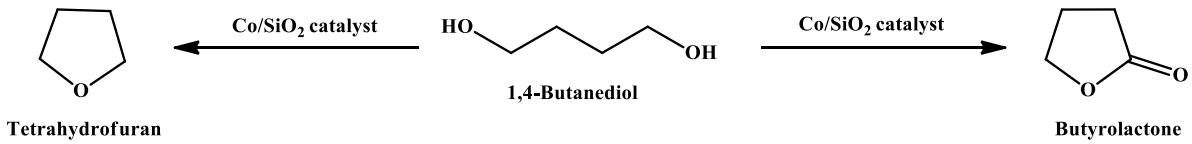

Scheme-I: Schematic illustration of 1,4-butanediol dehydrogenation on Co/SiO_2 catalysts

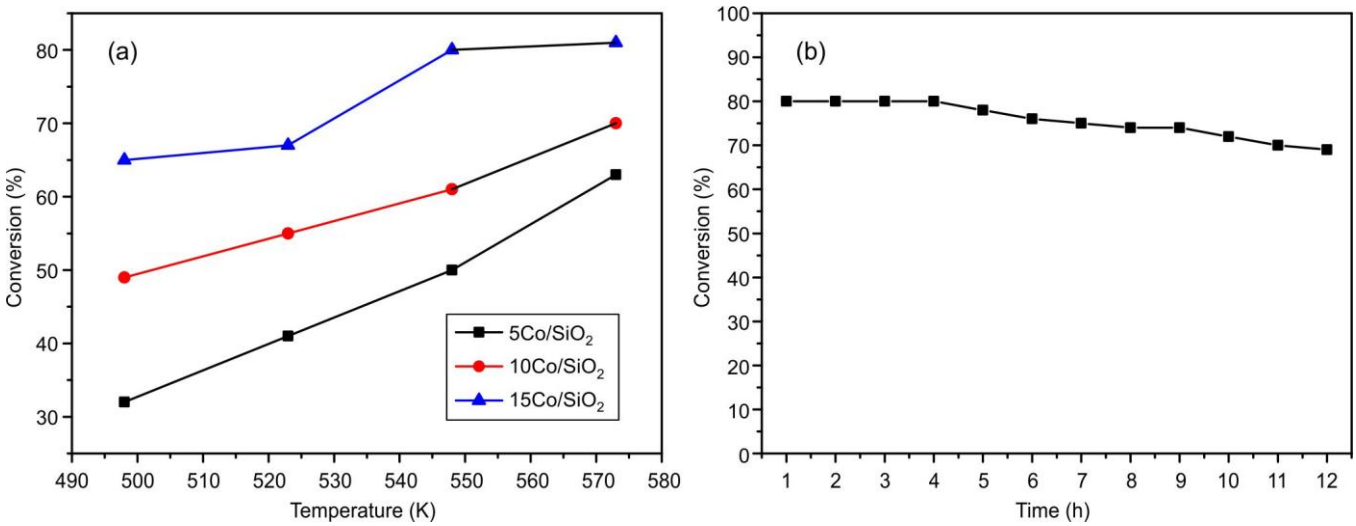

Fig. 4. Catalytic performance of Co/SiO_2 catalysts: (a) effect of reaction temperature on 1,4-butanediol conversion; and (b) time-on-stream stability study for 15Co/SiO_2 at 580 K

activity of 5Co/SiO_2 arises from stronger metal–support interactions, which hinder cobalt reduction and limit the number of accessible active sites across the investigated temperature range.

Product selectivity: The product distribution is governed by the competition between the dehydrogenation and dehydration pathways, which is strongly influenced by both cobalt loading and reaction temperature. Increasing the cobalt loading raises the density of metallic Co^0 sites, promoting C–H and O–H bond activation in 1,4-butanediol and favouring the formation of γ-butyrolactone through dehydrogenation followed by intramolecular cyclization. In contrast, tetrahydrofuran is formed *via* acid-catalyzed intramolecular dehydration, facilitated by the weak acidic silanol groups on the SiO_2 surface. Higher reaction temperatures slightly increase tetrahydrofuran selectivity as the dehydration pathway becomes kinetically more favourable.

For 5Co/SiO_2, the strong metal–support interaction limits the formation of metallic Co^0 sites, suppressing the dehydrogenation pathway and increasing the relative contribution of dehydration. As a result, the product distribution is determined by the balance between metallic Co^0 sites, which favour γ-butyrolactone, and the surface acidic sites of silica, which promote tetrahydrofuran formation. This balance can be effectively tuned by adjusting the cobalt loading and reaction temperature.

Reaction mechanism: The dehydrogenation of 1,4-butanediol over Co/SiO_2 is proposed to proceed through a sequence of surface-mediated elementary steps, as shown in **Scheme-I**. Initially, 1,4-butanediol adsorbs onto metallic Co^o sites through its hydroxyl groups, facilitating the activation of C–H and O–H bonds. The adsorbed molecule undergoes selective dehydrogenation to form 4-hydroxybutanal with the release of the first equivalent of H_2. This intermediate then undergoes rapid intramolecular cyclisation to produce a hemiacetal (lactol) intermediate, which is subsequently dehydrogenated to yield γ-butyrolactone, accompanied by the release of a second equivalent of H_2. This second dehydrogenation step is considered rate-limiting and is favoured by a high density of readily accessible Co^o sites with good reducibility. In parallel, 1,4-butanediol can undergo direct intramolecular dehydration on the weak acidic silanol groups of the SiO_2 support to form tetrahydrofuran, a pathway that becomes more significant at higher reaction temperatures and lower metallic cobalt site densities. The product distribution is therefore governed by the balance between metallic Co^o sites, which promote dehydrogenation to γ-butyrolactone, and the acidic surface sites responsible for dehydration. Increasing cobalt loading enhances the concentration of metallic Co^o sites after reduction, shifting the reaction toward γ-butyrolactone while suppressing the competing dehydration pathway.

Catalyst stability: Based on the catalytic activity results, the 15Co/SiO_2 catalyst was selected for a 12 h on-stream stability test under the optimized reaction conditions (Fig. 4b). The catalyst maintained 1,4-butanediol conversion between 85% and 69%, exhibiting only a gradual decline in activity throughout the reaction. This slight deactivation is likely associated with limited coke deposition on the active sites or partial surface oxidation of metallic Co^o during prolonged operation. The sustained catalytic performance demonstrates the good stability of the Co/SiO_2 catalyst under continuous-flow conditions, highlighting its potential for long-term dehydrogenation of 1,4-butanediol.

Comparison with literature: Previous studies provide valuable context for interpreting the present results, as cobalt has frequently been employed as a promoter in Cu-based catalysts for the dehydrogenation of 1,4-butanediol (Table-2). Reddy *et al*. [6] reported that the preparation method of Co–Cu/MgO catalysts strongly influence product selectivity by altering catalyst structure and metal dispersion, thereby affecting the balance between dehydrogenation and dehydration pathways. Kannapu *et al*. [7] subsequently demonstrated that cobalt incorporation improves both metal dispersion and copper particle distribution in Cu/MgO catalysts, with the optimized 10Co-20Cu-70MgO composition achieving γ-butyrolactone and aniline yields exceeding 90% in a tandem dehydrogenation–hydrogenation process. Recent studies on Cu-CuO-ZnO [15], Cu/SiO_2 [16] and Cu/SBA-15 [17] catalysts have highlighted the importance of catalyst composition, support characteristics and reactor configuration in enhancing catalytic performance. In contrast, the present Co/SiO_2 catalyst employs cobalt as the sole active phase, providing a simpler copper-free catalyst system. The catalytic performance can be tuned directly by adjusting the cobalt loading, which controls the density of accessible metallic Co^o sites, enabling simultaneous improvement in 1,4-butanediol conversion and γ-butyrolactone selectivity without the complexity of bimetallic or composite catalyst architectures.

Conclusion

Co/SiO_2 catalysts containing 5, 10 and 15 wt.% cobalt were successfully prepared by the incipient wetness impregnation method and evaluated for the vapour-phase dehydrogenation of 1,4-butanediol. Increasing the cobalt loading resulted in a gradual decrease in BET surface area due to the partial pore filling by Co_3O_4 particles, although the mesoporous structure of the silica support remained largely intact. XRD confirmed the formation of crystalline cubic-spinel Co_3O_4, with crystallite size increasing as the cobalt loading increased. H_2-TPR analysis showed that higher cobalt loading weakened the metal-support interaction and improved the reducibility of cobalt species, increasing the availability of catalytically active Co^o sites. Catalytic activity increased with both reaction temperature and cobalt loading, with 15Co/SiO_2 exhibiting the highest 1,4-butanediol conversion (≈80% at 580 K) while maintaining stable performance during 12 h of continuous operation. Product selectivity was controlled by the balance between metallic Co^o sites, which favoured γ-butyrolactone formation and the acidic silanol sites of the silica support, which promoted tetrahydrofuran formation. These results establish cobalt loading as an effective parameter for controlling catalyst structure, reducibility and product selectivity. The present study demonstrates that high-loading Co/SiO_2 catalysts provide an efficient and economically attractive route for the selective dehydrogenation of 1,4-butanediol to γ γ-butyrolactone under oxidant-free conditions. The combination of high activity, good stability and the use of an earth-abundant transition metal makes these catalysts promising candidates for the sustainable upgrading of biomass-derived diols to value-added chemicals.

CONFLICT OF INTEREST

The authors declare that there is no conflict of interests regarding the publication of this article.

TABLE-2
COMPARISON OF DEHYDROGENATION OF 1,4-BUTANEDIOL (BDO) OVER REPORTED CATALYSTS

Catalyst	Reaction conditions	Conversion (%)	Ref.
Cu/MgO	0.5 g catalyst, BDO = 1 mL h^{-1}, N_2 = 17 mL min^{-1}	83	[6]
Co–Cu/MgO	0.5 g catalyst, BDO = 1 mL h^{-1}, N_2 = 17 mL min^{-1}	91	[6]
Cu-CuO-ZnO	1.0 g catalyst, BDO = 1 mL h^{-1}, N_2 = 30 mL h^{-1}	100	[15]
10Cu/SBA-15	1.0 g catalyst, BDO = 1 mL h^{-1}, N_2 = 30 mL h^{-1}	100	[17]
Co/SiO_2	1.0 g catalyst, BDO = 1 mL h^{-1}, N_2 = 30 mL h^{-1}	80	Present study

DECLARATION OF AI-ASSISTED TECHNOLOGIES

During the preparation of this manuscript, the authors used an AI-assisted tool(s) to improve the language and no data, results or scientific conclusions were generated by AI. All analyses, interpretations and conclusions are the authors' own. The authors reviewed and edited the content and take full responsibility for the published work.

REFERENCES

1. S. Gundekari and K. Srinivasan, *ChemCatChem*, **11**, 1102 (2019); https://doi.org/10.1002/cctc.201801782
2. K.V. Athira, N.P. Nimisha and A. Sakthivel, *Chem. Commun*., **62**, 12443 (2026); https://doi.org/10.1039/d5cc06795b
3. K.N. Patil, D. Prasad, V.K. Manoorkar, J.T. Bhanushali, A.H. Jadhav and B.M. Nagaraja, *J. Ind. Eng. Chem.*, **106**, 142 (2022); https://doi.org/10.1016/j.jiec.2021.10.018
4. E. Kurniawan, S. Hosaka, M. Kobata, Y. Yamada and S. Sato, *Chemistry*, **5**, 406 (2023); https://doi.org/10.3390/chemistry5010030
5. X. Ren, M. Zhou, W. Yu, M. Zheng and Q. An, *Catalysts*, **14**, 297 (2024); https://doi.org/10.3390/catal14050297
6. K.H.P. Reddy, N. Anand, P.S.S. Prasad, K.S.R. Rao and B.D. Raju, *Catal. Commun.*, **12**, 866 (2011); https://doi.org/10.1016/j.catcom.2011.02.013
7. H.P.R. Kannapu, C.K.P. Neeli, K.S. Rama Rao, V.N. Kalevaru, A. Martin and D.R. Burri, *Catal. Sci. Technol.*, **6**, 5494 (2016); https://doi.org/10.1039/C6CY00397D
8. H. Liu, Y. Jiang, H. Zhao and Z. Hou, *J. Ind. Eng. Chem.*, **102**, 251 (2021); https://doi.org/10.1016/j.jiec.2021.07.008
9. M. Varkolu, H.B. Bathula, Y.W. Suh, D.R. Burri and S.R.R. Kamaraju, *Appl. Petrochem. Res.*, **8**, 153 (2018); https://doi.org/10.1007/s13203-018-0203-z
10. V. Mohan, V. Venkateshwarlu, C.V. Pramod, B.D. Raju and K.S.R. Rao, *Catal. Sci. Technol.*, **4**, 1253 (2014); https://doi.org/10.1039/C3CY01072D
11. V. Mohan, C.V. Pramod, M. Suresh, K.H. Prasad Reddy, B.D. Raju and K.S. Rama Rao, *Catal. Commun.*, **18**, 89 (2012); https://doi.org/10.1016/j.catcom.2011.11.030
12. M. Salavati-Niasari and A. Khansari, *C.R. Chim.*, **17**, 352 (2014); https://doi.org/10.1016/j.crci.2013.01.023
13. V. Dosarapu, S. Bandalla, M. Ravula, G.B. Bathula, S. Mavurapu, D. Shee, M. Varkolu, M. Baithy and C.S. Vasam, *Sustain. Energy Fuels*, **7**, 3609 (2023); https://doi.org/10.1039/D3SE00518F
14. Y. Ji, Z. Zhao, A. Duan, G. Jiang and J. Liu, *J. Phys. Chem. C Nanomater. Interfaces*, **113**, 7186 (2009); https://doi.org/10.1021/jp8107057
15. P. Gidyonu, A. Nagu, S. Gundekari and M. Varkolu, *Catal. Commun.*, **187**, 106870 (2024); https://doi.org/10.1016/j.catcom.2024.106870
16. M. Varkolu, S. Gundekari, P. Kumar, D. Hajjar and A.A. Makki, *Can. J. Chem. Eng.*, **103**, 5752 (2025); https://doi.org/10.1002/cjce.70082
17. M. Ashok Raju, P. Gidyonu, P. Nagaiah, M. Venkat Rao, B. David Raju and K.S. Rama Rao, *Biomass Convers. Biorefin.*, **9**, 719 (2019); https://doi.org/10.1007/s13399-019-00406-4